A two-way membrane-type micro-actuator with continuous deflections

2000 J. Micromech. Microeng. 10 387

(http://iopscience.iop.org/0960-1317/10/3/313)

J. Micromech. Microeng. **10** (2000) 387–394. Printed in the UK PII: S0960-1317(00)11449-4

A two-way membrane-type micro-actuator with continuous deflections

Chenpeng Hsu and Wensyang Hsu†

Department of Mechanical Engineering, National Chiao Tung University, 1001 Ta Hsueh Road, Hsinchu, Taiwan 30010, Republic of China

E-mail: whsu@cc.nctu.edu.tw

Received 31 January 2000

Abstract. This paper presents design, simulation, fabrication, and testing of a novel two-way micro-membrane actuator able to deflect in both upward and downward directions with continuous deflections. The design concept, to realize two-way continuous movement, is achieved by arranging different bimorph structures at different regions of the actuator with two kinds of boundary conditions. The actuator comprises of a square membrane with four bimorph beams and one central bimorph plate on it. The material (e.g. aluminum) on the top layer of the bimorph beams and plate has a larger thermal expansion coefficient than the material (e.g. silicon dioxide) of the membrane. The driving voltages in the two operating modes are both less than 3.5 V at about 350 mW maximum power consumption for an 1 mm^2 membrane actuator. The upward and downward deflections achieved up to 50 and 15 μm with maximum simulated temperatures less than 420 and 150 °C, respectively. A finite-element model is built to simulate the thermal mechanical behaviors that are compared with the experimental results. The design parameters influencing the deflections of the actuator are also discussed.

(Some figures in this article appear in colour in the electronic version; see www.iop.org)

1. Introduction

As one of the essential components in the micromechanical elements, micro-membrane actuators can be used for micropumps [1], valves [2], relays, switches [3], ink-jet heads [4], self-testing features for accelerometers [5] or pressure sensors [6]. Different principles, such as piezoelectric, electrostatic, thermal and electromagnetic have been used in the membrane actuators for various applications. Thermal actuators are usually simpler, more reliable and easier to construct. Thermal actuation schemes are generally based on either the linear/volume expansion or phase transformation of the materials. The minimum power consumption and thermal loss can be reduced through elaborated geometric and structural designs of the device and the appropriate choice of materials, which can enhance the efficiency. In addition, thermal actuation has been shown to provide significant displacement, force and moderate activation time due to the scale effect [7, 8].

For out-of-plane movement, most actuators can deflect in one direction only, with continuous deflections [2, 9, 10] or discontinuous deflections by a buckling effect [4]. Only a few actuators with two deflection directions have been reported. These two-way actuators are based on the mechanical bistability of the buckled beam or plate structures. The micromechanical bistable bridges using electrostatic forces to switch the states are used for the non-volatile memory cells and tunable acceleration switches [11,12]. Matoba *et al* [13] produced a mechanical bistable switching device actuated by the interactive forces of a 200 μm long buckling cantilever and a tension band achieved a vertically snapping action of ± 6 μm [13]. Also, a bistable buckled polyimide membrane of 3.3 mm diameter achieved a deflection of 120 μm in both directions with thermopneumatic actuation for the use of a microvalve [14]. Wagner *et al* [15] developed a bistable electrostatic membrane actuator module, with a pneumatic coupling operating in counteraction, achieved a deflection of ± 10 μm. However, they can only stay at two stable positions by snapping from one position to another in turn.

In this paper, an electro-thermally driven micro-membrane actuator able to deflect in both the upward and downward directions with continuous deflections is proposed. This novel design concept of two-way continuous movement is achieved by forming different bimorph structures at different regions of the actuator with two kinds of boundary conditions. While the bimorph beams are heated, the actuator will deflect from the initial rest state to the downward direction. In contrast, the heating of the central bimorph plate structure induces an upward flexing. The characteristics of the two operating modes with continuous deflections from

† Author to whom correspondence should be addressed.

an initial unactivated state to the other upward or downward deflecting state have not been found in other membrane actuators. This feature enables us to control the deflections and directions of the membrane optionally. Through finite-element analysis, geometric and structural parameters of the actuator influencing the deflections in two directions are discussed. In addition, experimental and testing results are discussed and compared with finite-element analysis.

2. Principle and concept design

2.1. Basic principle

The conventional thermal bimorph actuators can provide deflection or force due to the bending moment generated by the stresses induced from the interface of two components of a composite with different thermal expansion coefficients when the temperature changes. The theory of a bimorph strip under uniform heating was first investigated by Timoshenko in 1925 and the considerations in calculating the behavior of bimorph plates was also discussed [16]. The results obtained by this theory are useful in choosing the material combination and deciding on the layer thickness to maximize the bimorph effect. The analytical equation of the bimorph cantilever, as the simplified case of the bimorph strip, for the tip deflection and force as a function of temperature change was derived [17, 18]. Theoretical expressions described the behaviors of the bimorph membrane and the circular bimorph membrane subjected to a uniform temperature increase on the annular region under different boundary conditions [19]. For a clamped circular bimorph membrane with a material of a larger thermal expansion coefficient on the top layer, the deflection is downward; for a simply-supported membrane, the deflection is upward. However, the theoretical model is a composite membrane with only the annular region being heated, hence it is impractical in actual actuator design and fabrication.

In order to investigate the effects of different heating regions of a bimorph membrane with different boundary conditions, finite-element method (FEM) models are used. The FEM models comprise 1 mm $\times$ 1 mm SiO_2 square membranes, 2.8 μm thick, with an aluminum film, 1.8 μm thick, covering only the central square region or outer region of the SiO_2 membrane. The behavior of circular bimorph membranes is similar to the square bimorph membranes and hence it is not listed. In simulation, only the central square region or outer region covered with the aluminum film is subjected to a uniform temperature increase, 5 °C. Figure 1 demonstrates the relationships between the membrane deflections and heating regions with different boundary conditions. The lateral axis represents the ratio between the edge lengths of the central square region l and the membrane L, denoted by l/L. The arrows on the curves indicate the direction where the areas of the heating bimorph region increase. For membranes with Al films covering on the central region, the heating area increases as the ratio l/L approaches one. On the other hand, for membranes with Al films covering on the edge region, the heating area increases as the ratio l/L approaches zero. It is found that the simply-supported membranes deflect upward only, no matter where the heating region is, i.e. at the central

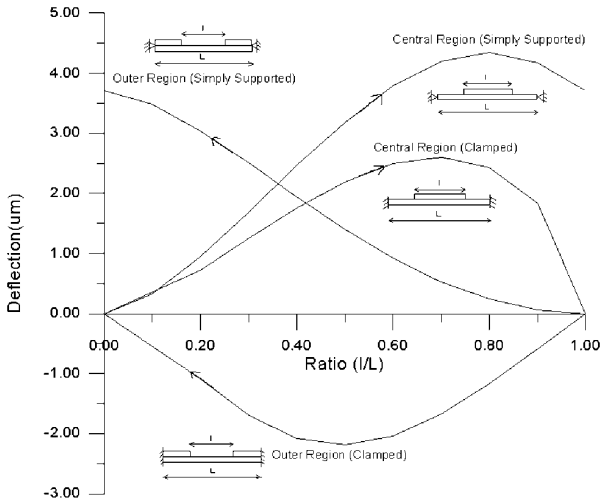

Figure 1. The effects of different heating regions of a square bimorph membrane with two kinds of boundary conditions. The central and outer region are subjected to a uniform temperature increase of 5 °C. The lateral axis represents the ratio between the edge lengths of the central square region l and the membrane L (=1 mm), denoted by l/L.

or outer area. In addition, in figure 1, it is shown that only a clamped membrane with a heating region at the outer area can provide downward deflection. Moreover, membranes with a heating region in the central area deflect upward only, regardless of the boundary conditions and the simply-supported membrane provides larger upward deflection than the clamped membrane. When the Al films cover the whole region, the deflection of the clamped membrane will reduce to zero if the induced thermal stress is less than the critical stress.

2.2. Concept design

In order to realize continuous two-way deflection, different bimorph structures with different boundary conditions are combined on different regions of a membrane. Figure 2 shows the schematic diagram of the proposed actuator. The actuator comprises a 1 mm^2 square composite membrane ($SiO_2/Si_3N_4/SiO_2$) with patterned aluminum films on the top layer. These aluminum films constitute four bimorph cantilever structures on the four sides of the membrane denoted by A, B, C, D; one central bimorph plate structure including the central area denoted by M; and four rectangular areas denoted by m1, m2, m3 and m4 at four corners of the membrane. The bimorph cantilever structures are rigidly connected with the substrate that can be regarded as one-end-clamped bimorph cantilevers subjected to the constraint of nonlinear spring forces at the periphery when the cantilevers are heated. Figure 3 demonstrates the downward operating mode of the membrane actuator by heating the bimorph cantilevers. The generated bending moments from the bimorph cantilevers force the membrane to deflect downwards. On the other hand, the central bimorph plate structure is connected with the substrate through the relatively thin-film members on the borders of the four corners, which can be treated as an approximation of the simply-supported boundary condition of the membrane. When the central bimorph plate structure is heated, as shown in figure 4, the

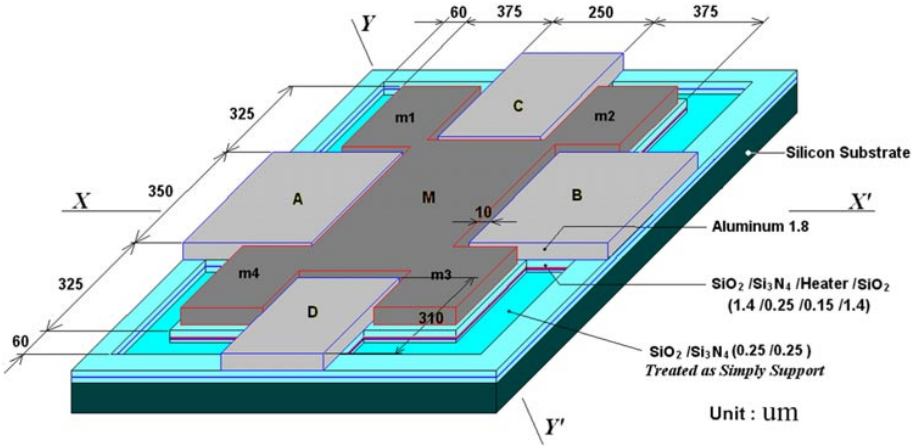

Figure 2. A schematic diagram of the two-way micro-membrane actuator, which defines the geometry.

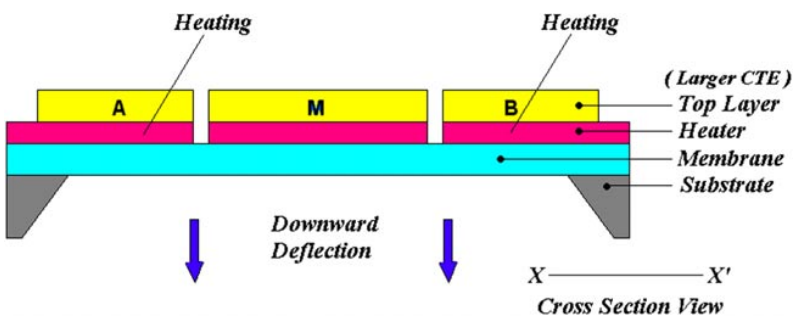

Figure 3. Downward operating mode of the two-way membrane actuator by heating the four bimorph cantilevers A, B, C and D (where C and D are not drawn here).

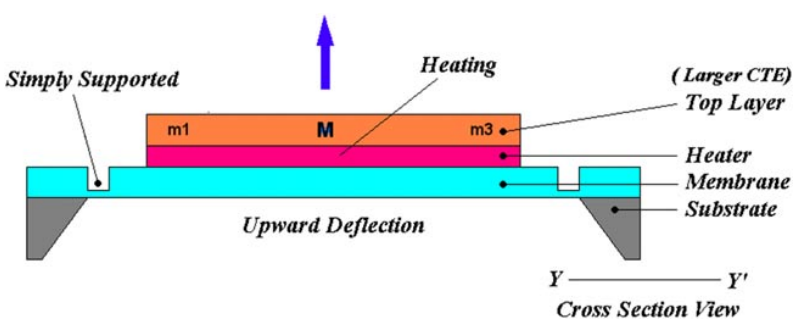

Figure 4. Upward operating mode of the two-way membrane actuator by heating the simply supported central bimorph plate structure M.

membrane will deflect upward due to the simply-supported boundary condition. Therefore, the deflections and deflecting directions can be controlled by heating different bimorph structures of the actuator i.e. the operating modes can be optionally controlled.

Taking the materials commonly used in the semiconductor technology and the bimorph effects into consideration, a combination of SiO_2 and Al is chosen. Due to the large compressive intrinsic stress of the SiO_2 film, the $SiO_2/Si_3N_4/SiO_2$ (1.4 μm/0.25 μm/1.4 μm) sandwich structure is used to serve as the membrane structure and to compensate the stress distribution through the thickness of the membrane. Other materials such as single-crystal silicon, polysilicon and silicon-rich nitride can be used instead of the SiO_2 as the membrane structure due to their good mechanical properties. Likewise, nickel and copper are good substitutes for the aluminum because of the higher melting points and stable characteristics over time. The materials on the borders of four corners are the composite of SiO_2/Si_3N_4 (0.25 μm/0.25 μm), which approximates the simply-supported boundary condition of the central bimorph plate structure. Heating of the bimorph structures is achieved by integrating meandered metal resistors embedded in the sandwich membrane structure and under the aluminum films in order to have uniform heating of the bimorph structures.

3. Numerical modeling

In the simulation of the two-way membrane actuator, a three-dimensional solid model was established to examine the thermal mechanical behaviors by using the finite-element analysis software ANSYS 5.3. Nonlinearities such as large

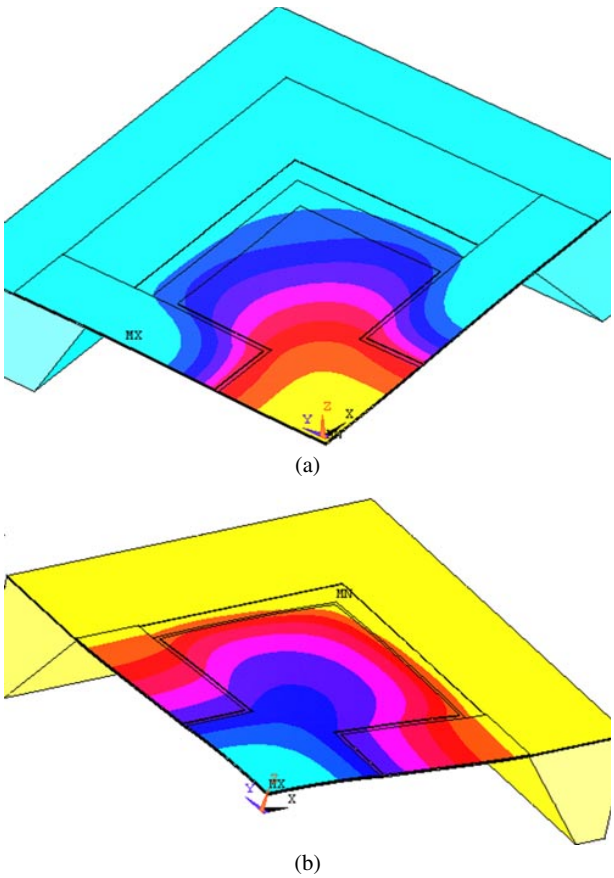

Figure 5. Deflections of the three-dimensional solid model used in finite-element analysis: (a) downward operation mode (b) upward operation mode.

deflection and stress stiffening were considered. In addition, heat conductivity, free convention and radiation were also considered. The steady-state temperatures and deflections of the membrane actuator are simulated by applying a heat generation rate per unit volume (W m^{-3}) to the metal resistor layers embedded in the composite membrane structure of the model. The simulation results are compared with the experimental results in a later section (see figure 11 below). Figures 5(a) and 5(b) show the deflections of the membrane actuator under upward and downward operation modes with an applied heat power of 100 mW. For upward operation mode, it is found that the temperature is uniformly distributed over the whole central bimorph plate structure and reaches about 420 °C at 350 mW heat power. However, for the downward operation mode, a strong temperature gradient can be found near the clamped end of the bimorph cantilever. The temperature along the bimorph cantilever increases nonlinearly from the fixed end to the tip and achieves 150 °C at 350 mW heat power. It is obvious that the thermal loss for downward operation is much greater than the upward operation. This is due to heat conduction from the clamped end of the bimorph cantilever to the silicon substrate and the heat absorption from the central bimorph plate structure. From analysis, the heat losses at the surfaces of the actuator by free convection, conduction and radiation to the air can be neglected in comparison with the heat losses from the bimorph cantilever to the silicon substrate.

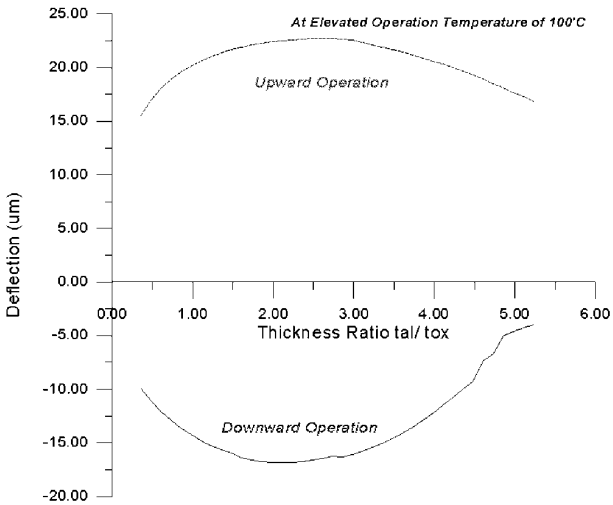

Figure 6. The influences of the thickness ratio t_{al}/t_{ox} on the upward and downward deflections at a constant elevated temperature of 100 °C for both operating modes. The width and length of the bimorph cantilever are both 250 μm; the dimension of the membrane actuator is 1 mm^2.

The influences of some design parameters on the mechanical performances of the membrane actuator are also simulated at a constant elevated temperature of 100 °C applied to the bimorph structures for both operating modes. Figure 6 shows the relationship between the thickness ratio t_{al}/t_{ox} and the deflections. The values of t_{al} and t_{ox} represent the thickness of the aluminum film and the total SiO_2 film thickness of the $SiO_2/Si_3N_4/SiO_2$ (1.4 μm/0.25 μm/1.4 μm) sandwich membrane structure, which is set to be a constant of 2.8 μm in the simulation. It indicates that the maximum upward deflection occurs at the thickness ratio $t_{al}/t_{ox} \sim 2.5$ and the maximum downward deflection occurs at the thickness ratio $t_{al}/t_{ox} \sim 2.0$, which means a thick Al film of 5.6–7.0 μm is required. However, the deposition of thick aluminum films by processes such as thermal evaporation or sputtering would be wasteful and expensive, therefore, a 1.8 μm thick Al film is chosen in the fabrication process.

In addition to the thickness ratio, the dimensions of the bimorph cantilever also affect the deflections of the membrane. In figure 7, 'w' denotes the width of the bimorph cantilever and the lateral axis represents the area percentage of the four bimorph cantilevers to the total membrane area. In simulation, the width of the bimorph cantilever w is set at several values of 150 μm, 200 μm, 250 μm, 300 μm and 350 μm and the total area of the membrane is set to be a constant value of 1 mm^2. For a given width w, the downward deflection increases with the areas of the cantilevers. However, the upward deflection becomes smaller when the area percentage of the bimorph beams increases. Therefore, the deflection stroke, the difference between upward and downward deflections, is almost invariant for the dimension given for the membrane actuator. For instance, the deflection stroke of the 1 mm^2 membrane actuator simulated here is 30±2.5 μm when it is elevated by 100 °C. In addition, a wider cantilever leads to larger upward and downward deflections. However, in order to avoid overlap between four beams, the width of the cantilever has a certain limitation.

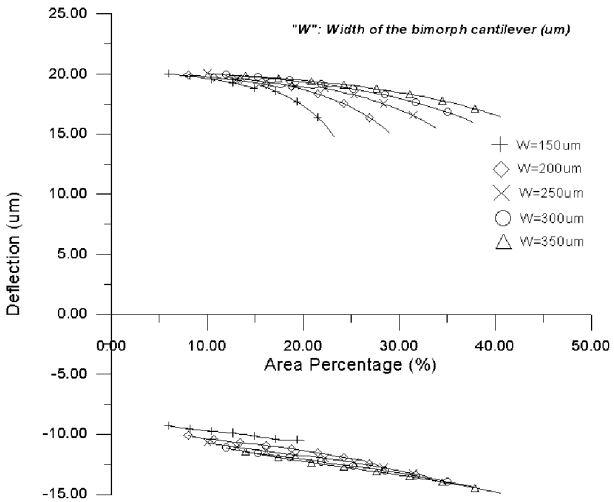

Figure 7. The relations of the upward and downward deflections and the area percentage of the bimorph cantilevers at a constant elevated temperature of 100 °C for both operating modes.

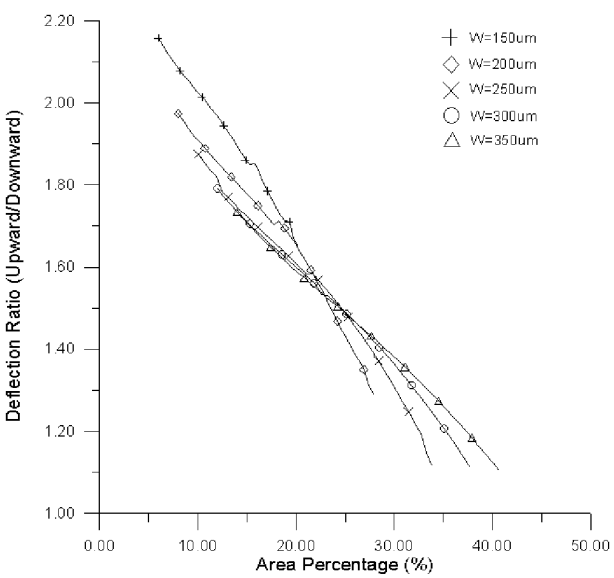

Figure 8. The deflection ratio is influenced by area percentage of the bimorph cantilevers with different widths at a constant elevated temperature of 100 °C for both operating modes.

Figure 8 shows the influences of the area percentage of the bimorph cantilevers on the deflection ratio, which is the ratio of upward deflection to downward deflection. The desired deflection ratio can be achieved by adjusting the width and/or the area percentage of the bimorph cantilevers. As shown in figure 8, increasing the area percentage of the bimorph cantilevers and/or widening the beam width can result in a larger downward deflection. However, from simulations, it is found that increasing of the area percentage of the bimorph cantilevers will reduce the flatness of the membrane to form a more spherical shape in both upward and downward operations. Furthermore, when the width of the bimorph cantilever is 250–300 μm, the membrane has better flatness; otherwise, the deformed shape of the membrane becomes more spherical in the central region. Therefore, a bimorph cantilever that is 250 μm long and 250 μm wide is chosen here.

4. Fabrication

The fabrication sequence is illustrated in figure 9. The complete process combining surface and bulk micromachining technology uses five photomasks. Surface micromachining is used to form the composite membrane structure comprising different material layers with different thicknesses. The membrane is then released by bulk micromachining.

The process begins with 1.4 μm thermal oxidation on a 4 inch double-side polished (100) silicon wafer. Subsequently, the 1.25 μm deep trenches are formed on the four corners of the membrane by the buffered oxide etchant (BOE) and a 0.25 μm thick low-pressure chemical vapor deposition (LPCVD) silicon nitride Si_3N_4 is then deposited (figures 9(a)–(c)). The thin composite members SiO_2/Si_3N_4 (0.25 μm/0.25 μm) on the four corners are more flexible relative to the whole membrane structure and can be treated as the simply-supported boundary condition of the membrane. Next, a positive photoresist, used as the lift-off masking layer, is spin coated and developed with a photomask. Then, the first 300 Å Cr layer and the second 1200 Å Au layer are deposited by electron beam evaporation (EBE) and patterned by a lift-off process to form the heating resistors of the actuator (figure 9(d)). Then an 1.4 μm thick plasma enhanced chemical vapor deposition (PECVD) SiO_2 film is deposited and patterned to isolate the metal heating resistors (figure 9(e)). The large compressive intrinsic stresses of the first thermal oxide film are compensated by the $SiO_2/Si_3N_4/SiO_2$ sandwich structure. Subsequently an 1.8 μm thick aluminum film is deposited by thermal evaporation and patterned (figure 9(f)). The aluminum patterns and the composite membrane structure form the actuating elements of the actuator: the bimorph cantilevers and the central bimorph plate structure. Finally, the SiO_2 film on the back side of the wafer is patterned to define the windows for the silicon back-side etching (figure 9(g)). A Teflon chuck is designed to protect the patterns on the front side of the wafer. Then the wafer is anisotropically etched in a time-controlled 30 wt% alkaline solution at 70 °C. After removing the Teflon chuck, cleaning in deionized water and drying the wafer in the air, the completed membrane actuator is obtained (figure 9(h) and 9(i)).

5. Experimental results and discussions

Experiments are conducted on a probe station with an optical microscope. We focus the optical microscope on the center of the membrane. The input power is recorded and the upward/downward deflections are measured by the focus/defocus method, which gives a measurement error of about ± 1 μm. Figure 10 is a scanning electron microscope (SEM) micrograph of the fabricated two-way micro-membrane actuator. Owing to the residual stresses induced in the fabrication process and the intrinsic stresses of the different materials, the initial downward displacements of about 5–10 μm are found in the center of the membranes.

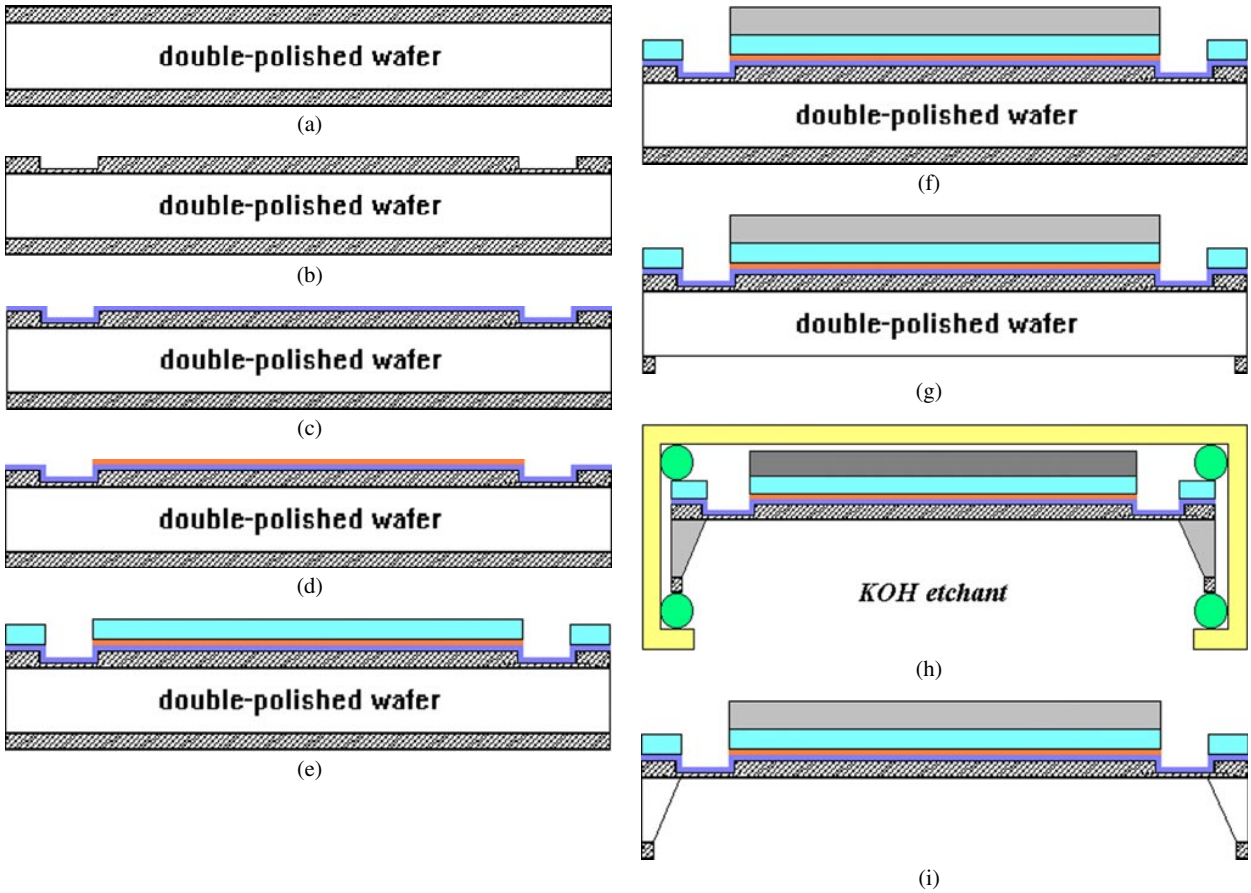

Figure 9. Schematic diagram of the fabrication process of the membrane actuator using surface and bulk micromachining. (a) Double-sided polished (100) silicon wafer is thermally grown with 1.4 μm thick SiO_2 layer. (b) The trenches on the borders are etched to the depth of 1.15 μm. (c) Deposited by LPCVD 0.25 μm of Si_3N_4. (d) Evaporated Cr/Au (300 Å/1200 Å) in sequence and define the metal heating resistors by a lift-off technique. (e) Deposited by PECVD 1.4 μm of SiO_2 and then pattern the PECVD SiO_2 on the borders. (f) Deposited a 1.8 μm thick aluminum layer and then pattern. (g) Etch the back-side SiO_2 layer by IR alignment. (h) Anisotropic etch the back side of the wafer with KOH etchant. (i) Remove the Teflon chuck.

This displacement could be improved by decreasing the thickness of aluminum films or by annealing the aluminum films to reduce the large tensile stresses that cause the whole membrane to deflect downwards.

The averaged testing results of the devices and simulation results are plotted in figure 11. The experimental results are smaller than the predictions of the simulations. This may be due to the initial downward curvature of the membrane, which makes the membrane stiffer. In addition, the mechanical properties are set to be independent of temperature in the simulation and the residual stress effect is not included in the three-dimensional solid model. It is also found that the difference between the testing results and the simulated results becomes more evident at an input power over 250 mW during upward operation. This phenomenon is due to the thermal buckling effect of the membrane that is not considered in the FEM model. The buckling effect is not found during downward operation even at the input power of up to 350 mW. This is due to the much lower operation temperature of the bimorph cantilever resulting from the thermal loss to the silicon substrate. For the same reason, it is found that the temperatures of the bimorph structures of the membrane under the two operating modes with the same input powers are different where upward operation achieves higher temperatures and therefore larger deflections than that of downward operation, and hence a larger deflection ratio is observed. At a 350 mW power consumption of the 3.5 V dc input voltage, the membrane actuator reaches a maximum upward deflection of 50 μm and a maximum downward deflection of 15 μm. When the input power exceeds 350 mW, the Al films on the central bimorph plate structure begin to melt during upward operation.

In experiments, the thermal responses of the membrane actuator cannot catch up with the electrical signals at 55 Hz input frequency. The amplitudes reduce as the input frequency increases. Photography of the membrane actuator under different operation conditions are shown in figure 12. The dark places in the photographs are the regions of the membrane with a curved shape, which result in the scattering of the projected light. It is observed that the central area of the membrane during downward operation is clear, however, it becomes darker during upward operation. Therefore, it is concluded that the shape of the membrane on the central area during downward operation is flatter than that during upward operation.

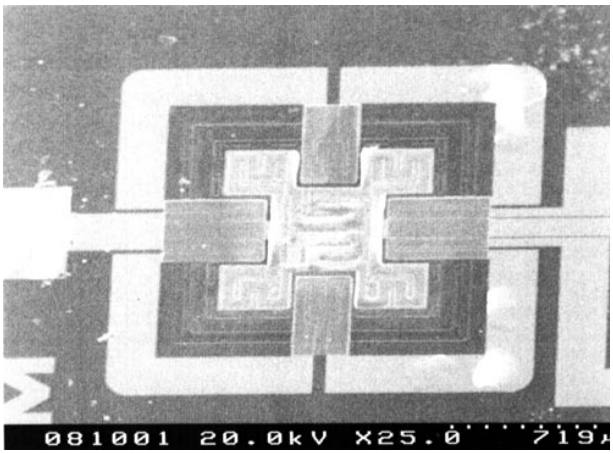

Figure 10. SEM micrograph of the fabricated two-way micro-membrane actuator.

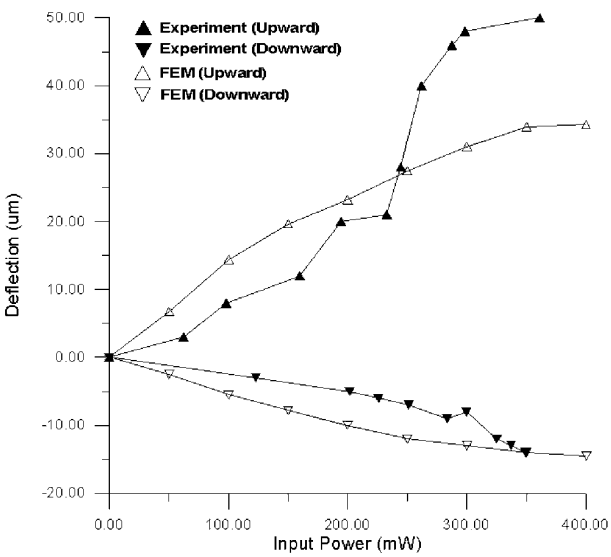

Figure 11. Experimental and simulation results of the upward and downward deflections on the center of the membrane actuator under different input powers. 1 mm^2 square membrane actuators, the width and length of the bimorph cantilever are both 250 μm.

6. Conclusions

A new design concept is demonstrated for an electro-thermally driven two-way membrane-type microactuator with continuous deflections by the arrangement of different bimorph structures with different boundary conditions on different regions of the actuator. The characteristics of two-way continuous deflection from an initial unactivated state to the other upward or downward deflecting state have not been found in other membrane actuators. This feature enables us to control the deflections and directions of the membrane optionally for possible applications such as two-way three-port active micro-valve and micro-flow control components with the advantage of smaller size. For the 1 mm^2 membrane actuator, the maximum upward and downward deflections of 50 and 15 μm are achieved, respectively, with less than 350 mW or 3.5 V dc input voltage. A three-dimensional finite-element solid model has been established to estimate the thermal–mechanical behaviors of the actuator. According to the simulation results of the design parameters, deflections of the membrane actuator can be modified by varying the thickness ratio of the composite structure. In addition, the deflection ratio is substantially affected by the area percentage of the bimorph cantilevers. Better bimorph beam widths are found to be 250–300 μm for an 1 mm^2 membrane, which shows better flatness on the central area of the membrane.

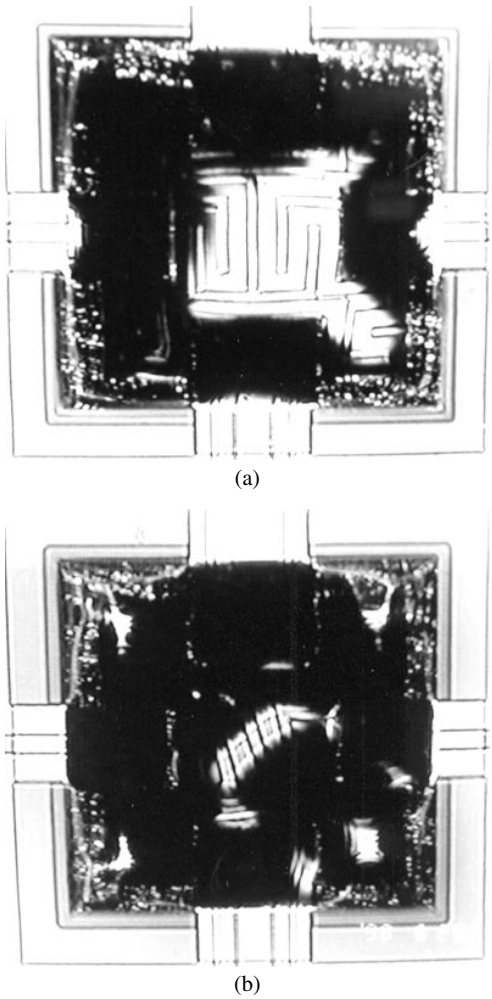

Figure 12. Optical photographs of the two-way micro-membrane actuator under different operation conditions: (a) downward deflection, (b) upward deflection.

Acknowledgments

This project was supported by the National Science Council of the Republic of China under grant number NSC87-2218-E-009-015 and the Materials Research and Development Center of CSIST. The authors also would like to thank the staff at the NCTU Semiconductor Research Center for providing technical support.

References

[1] Shoji S and Esashi M 1994 Microflow devices and systems *J. Micromech. Microeng.* **4** 157–71

[2] Jerman J H 1994 Electrically-activated normally-closed diaphragm valves *J. Micromech. Microeng.* **4** 210–16
[3] Hiltmann K, Keller W and Lang W 1999 Micromachined switches for low electric loads *Sensors Actuators* A **74** 203–6
[4] Hirata S, Ishii Y, Matoba H and Inui T 1996 An ink-jet head using diaphragm microactuator *IEEE Micro Electro Mechanical Systems Workshop* pp 418–23
[5] Pourahmadi F, Lee C and Petersen K 1992 Silicon accelerometer with new thermal self-test mechanism *IEEE Micro Electro Mechanical Systems Workshop* pp 122–5
[6] Puers R, Cozma A and Bruyker D D 1998 On the mechanisms in the thermally actuated composite diaphragms *Sensors Actuators* A **67** 13–17
[7] Pan C S and Hsu W 1997 An electro-thermally and laterally driven polysilicon microactuator *J. Micromech. Microeng.* **7** 7–13
[8] Lin Y S, Pan C S and Hsu W 1997 Thermally actuated bimorph microactuators *J. Chinese Soc. Mech. Eng.* **18** 525–31
[9] Tsao C C and Hsu W 1997 Micro membrane vibrator with thermally driven bimorph cantilever beams *Proc. SPIE* **3241** 195–205
[10] Zou Q, Sridhar U and Lin R 1999 A study on micromachined bimetallic actuation *Sensors Actuators* A **78** 212–19
[11] Hälg B 1990 On a micro-electro-mechanical nonvolatile memory cell *IEEE Trans. Electron Devices* **37** 2230–6
[12] Go J S, Cho Y H, Kwak B M and Park K 1996 Snapping microswitches with adjustable acceleration threshold *Sensors Actuators* A **54** 579–83
[13] Matoba H, Ishikawa T, Kim C J and Muller R S 1994 A bistable snapping microactuator *IEEE Micro Electro Mechanical Systems Workshop (Osio, Japan)* pp 45–50
[14] Goll C, Bacher W, Büstgens B, Maas D, Menz W and Schomburg W K 1996 Microvalves with bistable buckled polymer diaphragms *J. Micromech. Microeng.* **6** 77–9
[15] Wagner B, Quenzer H J, Hoerschelmann S, Lisec T and Juerss M 1996 Bistable microvalve with pneumatically coupled membranes *IEEE Micro Electro Mechanical Systems Workshop* pp 384–8
[16] Timoshenko S P 1925 Analysis of bi-metal thermostats *J. Opt. Soc. Am.* **11** 233–55
[17] Riethmüller W and Benecke W 1988 Thermally excited silicon microactuators *IEEE Trans. Electron Devices* **35** 758–62
[18] Chu W H, Mehregany M and Mullen R L 1993 Analysis of tip deflection and force of a bimetallic cantilever microactuator *J. Micromech. Microeng.* **3** 4–7
[19] Young W C 1989 *ROARK'S Formulas for Stress and Strain* (New York: McGraw-Hill)